Korean Journal of Radiology

KJR

Viscoelastic Property of the Brain Assessed With Magnetic Resonance Elastography and Its Association With Glymphatic System in Neurologically Normal Individuals

Bio Joo[1], So Yeon Won[2], Ralph Sinkus[3,4], Seung-Koo Lee[5]

[1]Department of Radiology, Gangnam Severance Hospital, Yonsei University College of Medicine, Seoul, Korea
[2]Department of Radiology, Kangbuk Samsung Hospital, Sungkyunkwan University School of Medicine, Seoul, Korea
[3]School of Biomedical Imaging and Imaging Sciences, King's College London, London, UK
[4]INSERM U1148, Laboratory for Vascular Translational Science, University Paris Diderot, Paris, France
[5]Department of Radiology and Research Institute of Radiological Science and Center for Clinical Image Data Science, Yonsei University College of Medicine, Seoul, Korea

Objective: To investigate the feasibility of assessing the viscoelastic properties of the brain using magnetic resonance elastography (MRE) and a novel MRE transducer to determine the relationship between the viscoelastic properties and glymphatic function in neurologically normal individuals.
Materials and Methods: This prospective study included 47 neurologically normal individuals aged 23–74 years (male-to-female ratio, 21:26). The MRE was acquired using a gravitational transducer based on a rotational eccentric mass as the driving system. The magnitude of the complex shear modulus $|G^*|$ and the phase angle φ were measured in the centrum semiovale area. To evaluate glymphatic function, the Diffusion Tensor Image Analysis Along the Perivascular Space (DTI-ALPS) method was utilized and the ALPS index was calculated. Univariable and multivariable (variables with $P < 0.2$ from the univariable analysis) linear regression analyses were performed for $|G^*|$ and φ and included sex, age, normalized white matter hyperintensity (WMH) volume, brain parenchymal volume, and ALPS index as covariates.
Results: In the univariable analysis for $|G^*|$, age ($P = 0.005$), brain parenchymal volume ($P = 0.152$), normalized WMH volume ($P = 0.011$), and ALPS index ($P = 0.005$) were identified as candidates with $P < 0.2$. In the multivariable analysis, only the ALPS index was independently associated with $|G^*|$, showing a positive relationship ($\beta = 0.300$, $P = 0.029$). For φ, normalized WMH volume ($P = 0.128$) and ALPS index ($P = 0.015$) were identified as candidates for multivariable analysis, and only the ALPS index was independently associated with φ ($\beta = 0.057$, $P = 0.039$).
Conclusion: Brain MRE using a gravitational transducer is feasible in neurologically normal individuals over a wide age range. The significant correlation between the viscoelastic properties of the brain and glymphatic function suggests that a more organized or preserved microenvironment of the brain parenchyma is associated with a more unimpeded glymphatic fluid flow.
Keywords: Brain; Magnetic resonance elastography; Glymphatic system; Neurodegenerative disease; Viscoelastic property

INTRODUCTION

According to the glymphatic system hypothesis, cerebrospinal fluid (CSF) enters the brain interstitial space via the aquaporin-4 channel on astrocyte endfeet within the perivascular space, mixes with the interstitial fluid (ISF)

and waste solutes, and then exits through the perivenous space, thereby clearing interstitial metabolic waste products [1-3]. Glymphatic system dysfunction is associated with various neurodegenerative disorders [1,4]. Therefore, various attempts have been made to evaluate the function of the glymphatic system in vivo, such as direct visualization of CSF movement using an intrathecal injection of a tracer or indirect assessment using the Diffusion Tensor Image Analysis Along the Perivascular Space (DTI-ALPS) method [5,6].

However, much remains to be elucidated regarding the glymphatic system. Given that the central function of the glymphatic system is the transport of fluids and solutes through the brain parenchymal microenvironment, a relevant research topic is a relationship between glymphatic function and the structural integrity or complexity of the brain parenchyma [7]. In this context, magnetic resonance elastography (MRE) is a promising new approach because of its ability to assess tissue viscoelastic properties in vivo, thus providing biomechanical information about the tissue microenvironment [8,9].

MRE is a phase-contrast magnetic resonance imaging (MRI) technique that can non-invasively measure in vivo tissue viscoelastic properties by measuring the three-dimensional (3D) shear wave displacement field produced during the propagation of acoustic waves generated by an external mechanical vibration source [10,11]. Although its application has been studied extensively in the liver, MRE has also been applied to the brain, suggesting that numerous neurological conditions associated with glymphatic dysfunction (e.g., Alzheimer's disease, Parkinson's disease, normal pressure hydrocephalus, multiple sclerosis, and brain aging) exhibit significant findings on MRE [11-18].

However, various aspects of MRE systems, such as driver systems for vibration delivery, image acquisition sequences, inversion algorithms, and terminology, have not yet been standardized [8]. Particularly regarding driver systems, a variety of approaches have been used for brain MRE [11]. Recently, a novel MRE vibration transducer based on a rotational eccentric mass was introduced and successfully tested in a pre-clinical phantom study and in vivo human liver MRE, producing highly accurate vibrational waves without second-harmonic vibrations and thus high-fidelity data [19,20]. Nevertheless, the application of the MRE system to the brain warrants further research.

We hypothesized that 1) the application of the MRE system to the brain using the novel transducer is feasible, and its normative data may be useful for future applications of the MRE system in patients with neurological diseases, and 2) a comprehensive evaluation of glymphatic function and viscoelastic properties of the brain may reveal significant correlations, ultimately offering valuable insights into age-related neurodegeneration.

Therefore, this study aimed to investigate the feasibility of assessing the viscoelastic properties of the brain using MRE and a novel MRE transducer and to determine the relationship between the viscoelastic properties of the brain measured by MRE and glymphatic function assessed using the DTI-ALPS method in neurologically normal individuals with a wide age range.

MATERIALS AND METHODS

Study Participants

This prospective study was approved by Severance Hospital Institutional Review Board (4-2019-0874) and was conducted in accordance with the Declaration of Helsinki. Informed consent was obtained from all the participants.

We screened 63 volunteers aged 20–79 years between October 2019 and January 2022. The recruitment process ensured that the number of participants in each age group was similar. The eligibility criteria were as follows: 1) age 20–79 years, 2) normal cognitive status, and 3) no history of neurological or psychiatric disorders. The exclusion criteria were 1) Mini-Mental State Examination score $\leq$ 25; 2) history of neurological disease; 3) diseases or findings that may increase bleeding risk (such as an intracranial aneurysm); 4) significantly abnormal findings on brain MRI (such as brain tumor); 5) scalp or skull lesions that hamper transducer placement; 6) general contraindications for MRI such as an implanted pacemaker); and 7) severe image artifacts or incomplete image acquisition. Although it has been proven that vibrations from the MRE transducer are safe for brain evaluation, abnormalities with bleeding tendencies were excluded from this study to eliminate the potential risk of vibration-induced adverse effects, such as aneurysm rupture [21]. Of the 63 participants, two were excluded due to overt intracranial aneurysm, six due to infundibulum indistinguishable from the aneurysm, one due to incidental meningioma, one due to old intracerebral hemorrhage, one due to capillary telangiectasia, and five due to severe artifacts. Finally, 47 participants (median age, 49 years [interquartile range, 34–62 years]; range, 23–74 years; male:female ratio, 21:26) were enrolled (Table 1). Figure 1 shows a flowchart of the recruitment process.

Image Acquisition

All scans were conducted between 10:00 a.m. and 2:00 p.m., following sufficient sleep to eliminate the possibility of diurnal variation, using a 3-Tesla system (Ingenia, Philips Medical Systems) with a 32-channel receiver head coil. Each scan comprised both brain MRI and MRE and was obtained in a single session. Brain MRI included 3D T1-weighted imaging (T1WI), 3D fluid-attenuated inversion recovery imaging (FLAIR), 3D time-of-flight MR angiography (TOF MRA), DTI, and susceptibility-weighted imaging (SWI). MRE was performed only after an on-site neuroradiologist confirmed that the exclusion criteria were not met based on the brain MRI findings. Detailed imaging parameters of brain MRI are summarized in the Supplementary Methods.

MRE was acquired using a gradient-recalled echo sequence with a Hadamard encoding scheme using a gravitational

transducer based on a rotational eccentric mass as the driver system [19,20]. The motor and controller units of the driver system are located in the MRI control room, and a flexible rotating shaft connects the motor unit to a gravitational transducer. The transducer was firmly fastened to the volunteer's head with a hair band and randomly assigned to either the right or left temporal region. A 1-cm thick gel pad ergonomically shaped according to the contour of the head was attached to the transducer to enhance comfort. The MRE scan covered the centrum semiovale region of the brain with the uppermost point on the upper boundary of the corpus callosum at the lowest slice level. Detailed imaging parameters of the brain MRE are summarized in the Supplementary Methods. Figure 2 shows the MRE driver system and the image acquisition.

Postprocessing

The post-processing pipeline is described in detail in the Supplementary Methods, and its graphical representation is shown in Supplementary Figure 1. After processing of MRE data using a finite element method-based inversion algorithm [22], maps of the following viscoelastic parameters were obtained: storage modulus G', loss modulus G", the magnitude of the complex shear modulus |G*|, and phase angle φ, where $|G^*| = \sqrt{G'^2 + G''^2}$ and $\varphi = \arctan\left(\frac{G''}{G'}\right)$. Of the four viscoelastic parameters, the magnitude of the complex shear modulus |G*| and phase angle φ were used for further analysis.

After automated segmentation of the brain parenchyma and white matter hyperintensity (WMH) using Statistical Parametric Mapping software (SPM12) and the LST toolbox, brain parenchymal volume and normalized WMH volume (ratio of the WMH volume to the total brain parenchymal volume) were calculated for subsequent analyses [23]. Next, the brain parenchymal mask was divided into right and left sides with respect to the brain midline to evaluate the influence of the transducer position on the measurement of viscoelastic parameters.

The ALPS index was estimated as described in a previous publication [6]. Three regions of interest (ROIs) were manually placed in the areas of projection, association, and subcortical neural fibers at the level of the lateral ventricle on color fractional anisotropy DTI maps by referring to SWI images. All the individuals were right-handed; hence, the ROIs were placed in the dominant left hemisphere. ROI placement was conducted by a neuroradiologist who was unaware of the MRE findings.

Table 1. Demographic Characteristics of Study Participants (n = 47)

Parameters	Values
Sex	
Male	21 (44.7)
Female	26 (55.3)
Median age (range; IQR), yr	49 (23–74; 34–62)
Number of participants by age group	
20–29 yr	7 (14.9)
30–39 yr	12 (25.5)
40–49 yr	5 (10.6)
50–59 yr	8 (17.0)
60–69 yr	11 (23.4)
70–79 yr	4 (8.5)

Data are the number of patients with percentage in parentheses unless specified otherwise. As the Shapiro–Wilk test rejected normality for age, values were reported as median values and interquartile ranges. IQR = interquartile range
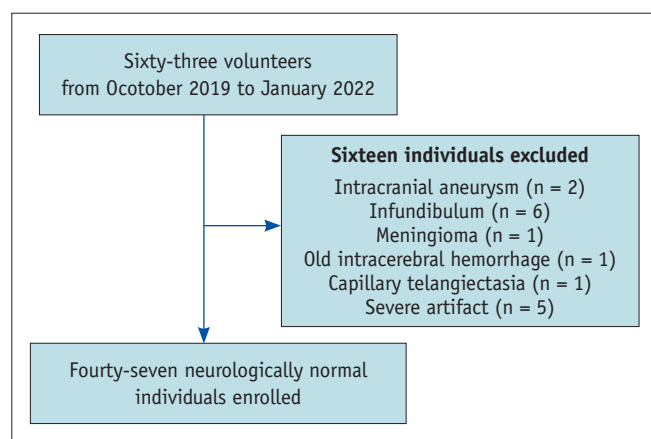
Fig. 1. Flow chart of volunteer recruitment.
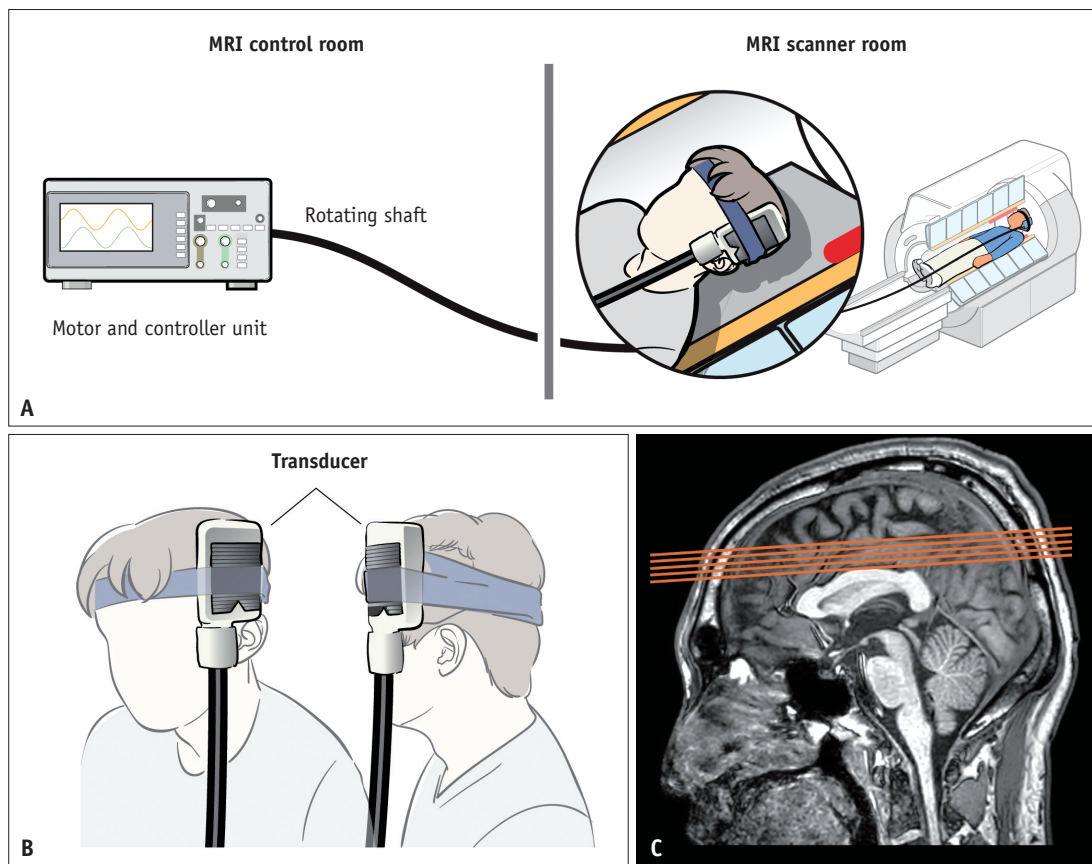
Fig. 2. Schematic diagram of the driver system and magnetic resonance elastography (MRE) acquisition. **A:** The transducer is connected to the motor and controller unit in the magnetic resonance imaging (MRI) control room through a rotating shaft. **B:** An example of the positioning of the transducer. The transducer was firmly fastened to either the right or left temporal region of the volunteer's head. **C:** Scan coverage of the MRE. The MRE scan covered the centrum semiovale region of the brain.

Statistical Analysis

Descriptive statistics for each viscoelastic parameter were reported. Univariable analyses with variables including age, sex, brain parenchymal volume, normalized WMH volume, and ALPS index were conducted to identify candidate factors to be included in the multivariable analysis of the association with the viscoelastic parameters ($|G^*|$ and φ) as the dependent variable. Multivariable linear regression analyses were conducted with variables ($P < 0.2$ in the univariable analyses) to assess independent relationships. The variance inflation factor (VIF) was calculated to determine the degree of multicollinearity. Finally, to investigate possible discrepancies in the measurement of viscoelastic parameters between the ipsilateral and contralateral sides with respect to the transducer position, the respective mean values of both sides were compared for each viscoelastic parameter using a paired *t*-test. Statistical significance was set at $P < 0.05$. Statistical analyses were performed using MedCalc Software (version 9.3.6.0; MedCalc).

RESULTS

Brain MRE data were successfully acquired for all enrolled volunteers. Vibrations were well tolerated by all individuals, with no reports of illness or pain. The mean ± standard deviation of the magnitude of the complex shear modulus $|G^*|$ and phase angle φ for all participants were 1.604 ± 0.165 kPa and 0.301 ± 0.032 rad, respectively. Table 2 summarizes the measurement statistics for all the participants by age group.

Univariable and Multivariable Analysis for the Magnitude of the Complex Shear Modulus $|G^*|$

Regarding the univariable analysis for $|G^*|$, age ($\beta = -0.004$, $P = 0.005$), brain parenchymal volume ($\beta < 0.001$, $P = 0.152$), normalized WMH volume ($\beta = -13.80$, $P = 0.011$), and ALPS index ($\beta = 0.385$, $P = 0.005$) were identified as candidates with $P < 0.2$. However, on multivariable analysis with those covariables, only the ALPS index was

independently associated with $|G^*|$, showing a positive relationship ($\beta = 0.300$, $P = 0.029$). All VIF values were less than 2 (Table 3, Fig. 3).

Univariable and Multivariable Analysis for the Phase Angle φ

For φ, normalized WMH volume ($\beta = -1.624$, $P = 0.128$) and ALPS index ($\beta = 0.064$, $P = 0.015$) were identified as candidates for multivariable analysis. However, only the ALPS index was independently associated with the phase angle φ on the multivariable analysis ($\beta = 0.057$, $P = 0.039$) (Table 4, Fig. 3).

The Influence of Transducer Position on the Measurement of Viscoelastic Parameters

Transducers were placed on the right and left sides of 24 and 23 participants, respectively. There was no significant difference between the ipsilateral and contralateral sides regarding transducer position for any viscoelastic parameter ($|G^*|$: $P = 0.954$; φ: $P = 0.698$) (Supplementary Table 1). Representative cases are shown in Figure 4.

DISCUSSION

In the current study, viscoelastic properties of the brain—the magnitude of the complex shear modulus $|G^*|$ and phase angle φ—were measured by the MRE system using a gravitational transducer as a driver system. Our study showed that glymphatic function, measured using the ALPS index, was independently associated with $|G^*|$ and φ when adjusted for other cofactors including age, WMH volume, and brain parenchymal volume. Moreover, the measurement of brain viscoelastic properties was independent of the transducer placement (ipsilateral or contralateral).

Currently, a driver system with a pneumatic actuator and head pillow is widely used in brain MRE because it is the only available commercial driver system [8]. However, potential errors in the reconstruction of biomechanical properties have been raised regarding the system, such as a decrease in the vibration amplitude or upper harmonic-related inaccuracies [19]. In this context, a novel MRE driver system based on a rotational eccentric mass, termed a gravitational transducer, was recently introduced and proven to produce highly accurate vibrational waves without second-harmonic vibrations and to be accurately phase-locked with an MRE sequence [19]. A recent study showed that the system was robust in terms of repeatability

Table 2. Summary Statistics of Measurements of All Participants and Participants by Age Group

Participants	$|G^*|$, kPa	φ, rad	Brain Parenchymal Volume, mL	Normalized WMH Volume	ALPS Index
All participants	1.604 ± 0.165	0.301 ± 0.032	1195.59 ± 132.99	4.571×10^{-4} (1.007×10^{-4}–1.690×10^{-3})	1.544 ± 0.174
20–29 yr	1.711 (1.508–1.751)	0.317 (0.293–0.330)	1200 (1157–1256)	0.000 (0.000–1.592×10^{-4})	1.649 (1.500–1.680)
30–39 yr	1.657 (1.523–1.767)	0.303 (0.291–0.322)	1329 (1175–1367)	8.500×10^{-5} (2.535×10^{-5}–4.734×10^{-4})	1.564 (1.498–1.651)
40–49 yr	1.617 (1.481–1.736)	0.305 (0.274–0.305)	1222 (1199–1311)	2.146×10^{-4} (1.216×10^{-4}–2.322×10^{-4})	1.400 (1.310–1.480)
50–59 yr	1.591 (1.511–1.700)	0.311 (0.308–0.327)	1112.8 (1076.8–1135.7)	6.191×10^{-4} (2.716×10^{-4}–1.999×10^{-3})	1.667 (1.543–1.754)
60–69 yr	1.543 (1.434–1.615)	0.308 (0.282–0.317)	1177.1 (1084.2–1239.4)	1.153×10^{-3} (9.160×10^{-4}–2.564×10^{-3})	1.557 (1.489–1.627)
70–79 yr	1.440 (1.379–1.521)	0.274 (0.254–0.287)	1015.1 (994.2–1072.9)	1.154×10^{-2} (9.909×10^{-3}–1.483×10^{-2})	1.281 (1.254–1.332)

Data are mean ± standard deviation or median (interquartile range). WMH = white matter hyperintensity, ALPS = analysis along the perivascular space

Table 3. Univariable and Multivariable Linear Regression Analyses for Magnitude of the Complex Shear Modulus |G*| in kPa

Variable	Univariable		Multivariable		
	β	P	β	P	VIF
Sex	0.018	0.722			
Age, yr	-0.004	0.005	-0.002	0.230	1.814
Brain parenchymal volume, mL	< 0.001	0.152	< 0.001	0.537	1.313
Normalized WMH	-13.80	0.011	-4.751	0.440	1.532
ALPS index	0.385	0.005	0.300	0.029	1.147

VIF = variance inflation factor, WMH = white matter hyperintensity, ALPS = analysis along the perivascular space
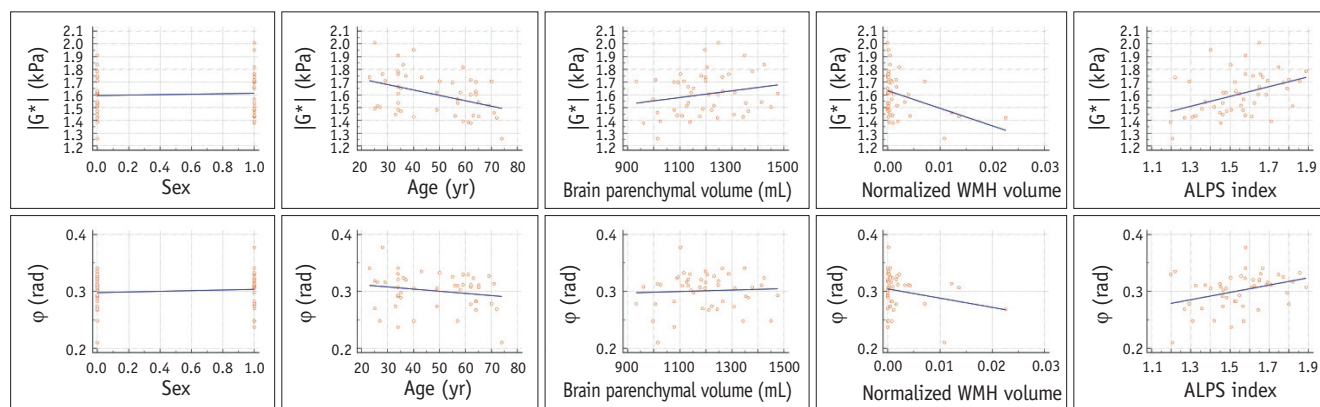
Fig. 3. Scatter diagrams and univariable analyses of the magnitude of the complex shear modulus |G*| (upper row) and phase angle φ (lower row) with age, sex, brain parenchymal volume, normalized white matter hyperintensity (WMH) volume, and analysis along the perivascular space (ALPS) index.

Table 4. Univariable and Multivariable Linear Regression Analyses for the Phase Angle φ in rad

| Variable	Univariable		Multivariable		
	β	P	β	P	VIF
Sex	0.006	0.535			
Age, yr	-0.000	0.202			
Brain parenchymal volume, mL	< 0.001	0.718			
Normalized WMH	-1.624	0.128	-0.898	0.404	1.115
ALPS index	0.064	0.015	0.057	0.039	1.115

VIF = variance inflation factor, WMH = white matter hyperintensity, ALPS = analysis along the perivascular space

and reliability [24]; however, only 15 volunteers with a narrow age range (21–33 years) were included. This study is the first to use the MRE driver system in individuals across a broad age range for brain MRE. We demonstrated that the transducer position had no significant effect on the assessment of the viscoelastic properties of the brain. These findings provide valuable information about normative age-related changes for future applications of the transducer in brain MRE in patients with neurological diseases.

Our study reported slightly lower values for viscoelastic parameters, in contrast to previous brain MRE studies. According to a systematic review, where the viscoelastic parameters were converted to shear stiffness μ [μ = 2

$|G*|^2/(G'+|G*|)]$ and loss tangent (tangent of the phase angle φ) to standardize results between different research groups, the mean shear stiffness and loss tangent of brain MRE at 50 Hz were 2.07 ± 0.42 kPa and 0.41 ± 0.06 rad, respectively [11]. In our study, the corresponding values were 1.708 ± 0.187 kPa and 0.310 ± 0.032 rad, respectively. This discrepancy may be attributed to differences in the brain regions imaged or MRE acquisition techniques. Further studies, including various MRE techniques, are warranted to set a reference range of viscoelastic parameters for the brain and, ultimately, to establish a standard brain MRE protocol.

The magnitude of the complex shear modulus |G*| is
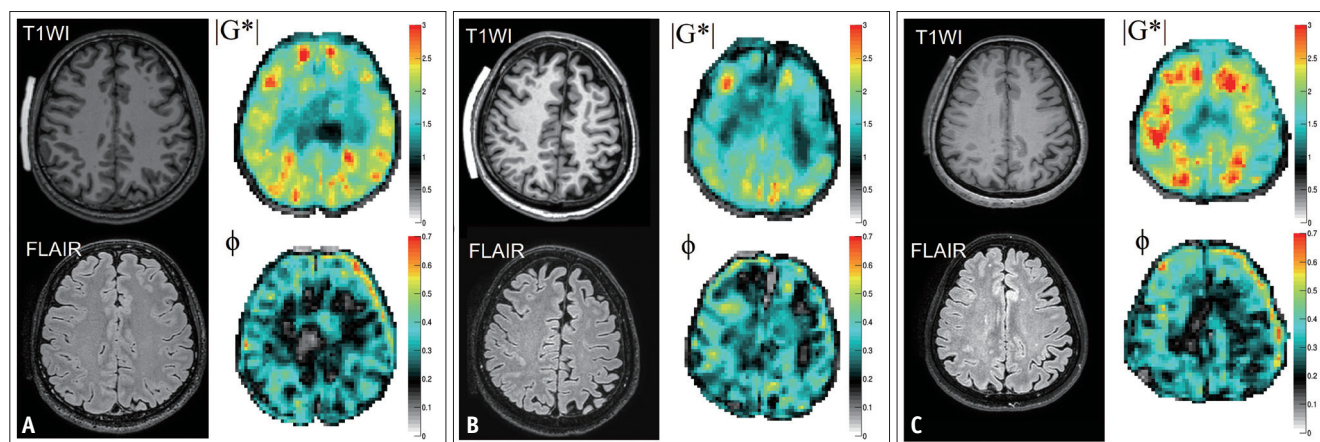
Fig. 4. Representative axial T1-weighted imaging (T1WI), fluid-attenuated inversion recovery imaging (FLAIR), and viscoelastic maps of a 34-year-old male **(A)**, a 70-year-old male **(B)**, and a 62-year-old female participant **(C)**. The mean values of |G*|, φ, brain parenchymal volume, normalized white matter hyperintensity volume, and analysis along the perivascular space (ALPS) index were as follows: **A:** 1.783 kPa, 0.307 rad, 1378.51 mL, 2.3221×10^{-4}, and 1.8883, respectively; **B:** 1.516 kPa, 0.327 rad, 1231.5 mL, 1.8269×10^{-3}, and 1.2926, respectively; **C:** 1.718 kPa, 0.277 rad, 1007.81 mL, 1.638×10^{-3}, and 1.8006, respectively. The participant in **(A)** showed a higher |G*| and ALPS index than the participant in **(B)**. Note that although the participant in **(C)** was relatively old, she demonstrated a relatively high |G*| and ALPS index. The bright material on the participants' right side on T1WI is the gel pad attached to the transducer.

regarded as a primarily tissue stiffness-related metric, whereas the phase angle φ is regarded as a primarily tissue viscosity-related metric [25]. We found in the univariable analysis that only |G*| was associated with age, whereas φ was not. This result is in concordance with previous reports, where only primarily tissue stiffness-related metrics, such as springpot-parameter μ or shear stiffness, showed a significant association with age, whereas primarily viscosity-related metrics, such as springpot-parameter α or damping ratio, did not [14,15,17]. The precise molecular and cellular conditions underlying changes in viscoelastic properties measured by MRE remain unclear. Based on previous studies, it is believed that primarily tissue stiffness-related metrics relate more to the mechanical backbone, which is largely dependent on tissue composition and/or myelination in the brain, whereas primarily viscosity-related metrics relate more to the complexity of the tissue architecture, which is attributed to the arrangement of axonal fibers and/or interneuronal connections [11,14,25-32]. In this context, our findings can be interpreted as preclinical tissue composition change (such as glia/neuron ratio) during normal aging but without severe degradation of the tissue geometry or architecture, which was also not apparent with structural MRI.

This is the first study to investigate the relationship between brain viscoelastic parameters and glymphatic function. The ALPS index is a measure of transependymal perivascular space water movement relative to that along

projection and association fibers and has been considered a promising biomarker of glymphatic function in various neurological conditions [5,6,33-36]. We found that a lower ALPS index was associated with lower values of both |G*| and φ, even after adjusting for age and age-related cofactors. Therefore, we can infer that glymphatic function is associated with the biomechanical properties of the brain parenchymal microenvironment, not only in terms of tissue composition but also tissue organization. Although direct evidence regarding this association at the molecular or histological levels is limited, one possible explanation is brain tissue deformability. Kedarasetti et al. [37] reported the deformability of brain tissue in response to arteriolar pulsations in the perivascular space. If the brain tissue deforms significantly due to a loss of tissue stiffness, kinetic energy may be removed from the CSF, resulting in decreased fluid flow and a lower ALPS index [7]. Another possible explanation is myelination in the parenchymal microenvironment of the brain. A recent study suggested a relationship between the integrity of myelination and the regulation of ISF drainage and substance transport in the extracellular space of the brain [38]. Given that |G*| decreases demyelination and global extracellular matrix destruction [29], this may explain the link between glymphatic function and changes in the brain's viscoelastic properties, which may not be solely due to aging. In addition, early stage brain microenvironmental alterations in cerebral small vessel disease that are not

discernible on other MRI sequences can be detected by MRE, thus explaining the association between |G*| and the ALPS index, even after adjusting for WMH volume. In this respect, this study provides useful insights into bridging the gap between numerous neurological conditions and the glymphatic hypothesis by directly demonstrating the relationship between glymphatic dysfunction and changes in brain viscoelastic properties. However, additional molecular and histological studies are required to fully understand the relationship between the viscoelastic properties of the brain and glymphatic function.

MRE is associated with numerous neurological conditions such as brain tumors, neurodegeneration, demyelination, trauma, brain aging, and even memory function [11,31]. In particular, the strong relationship between the viscoelastic properties of the hippocampus and relational memory performance is thought to be closely related to our findings, given that cognitive performance is significantly associated with the glymphatic function [1,31]. In this context, brain MRE may be a clinically useful imaging marker not only for neurodegeneration but also for functional assessment following neurological rehabilitation [9].

This study had several limitations. First, we obtained MRE images only for the centrum semiovale region with approximately 15-mm thick coverage. Although the applied vibration with a scan time of 2 min 20 s was tolerable in all volunteers, possible discomfort regarding the vibration was considered and minimized, resulting in a limited coverage size. Moreover, the spatial resolution of 2.75 x 2.75 x 3.14 mm³ of the MRE imaging may have been relatively low for the complete evaluation of differences in viscoelastic properties between the gray and white matter. Further investigation with whole-brain coverage, higher spatial resolution, and reduced scan time is required for clinical practice. The levels of MRE acquisition and ALPS index analysis were different. The MRE scan was obtained at the centrum semiovale, whereas the ALPS index was analyzed at the level of the lateral ventricle, which was slightly lower than the MRE acquisition level. However, the ALPS index has been suggested as an imaging marker that can reflect the glymphatic function of the entire brain and not only the periventricular region. Therefore, we believe that the difference in the image analysis level does not diminish the significance of our findings. Finally, the reproducibility of the MRE system was not tested. However, a recent study found that brain MRE using the same transducer showed robust repeatability and reliability [24]. However, future studies using various imaging systems and manufacturers are required to validate their reliability and reproducibility.

In conclusion, brain MRE using a gravitational transducer as a source of vibration is feasible in neurologically normal individuals over a wide age range. The significant correlation between the viscoelastic properties of the brain and glymphatic function suggests that a more organized or preserved microenvironment of the brain parenchyma is associated with a more unimpeded glymphatic fluid flow.

Supplement

The Supplement is available with this article at https://doi.org/10.3348/kjr.2022.0992.

Availability of Data and Material
The datasets generated or analyzed during the study are available from the corresponding author on reasonable request.

Conflicts of Interest
The authors have no potential conflicts of interest to disclose.

Author Contributions
Conceptualization: Seung-Koo Lee. Data curation: Bio Joo, So Yeon Won. Formal analysis: Bio Joo. Investigation: Seung-Koo Lee. Methodology: Ralph Sinkus. Resources: Ralph Sinkus. Software: Ralph Sinkus. Supervision: Seung-Koo Lee. Validation: Bio Joo. Visualization: Bio Joo. Writing—original draft: Bio Joo. Writing—review & editing: Seung-Koo Lee.

ORCID iDs
Bio Joo
   https://orcid.org/0000-0001-7460-1421
So Yeon Won
   https://orcid.org/0000-0003-0570-3365
Ralph Sinkus
   https://orcid.org/0000-0002-6093-1654
Seung-Koo Lee
   https://orcid.org/0000-0001-5646-4072

REFERENCES

1. Rasmussen MK, Mestre H, Nedergaard M. The glymphatic pathway in neurological disorders. *Lancet Neurol* 2018;17:1016-1024

2. Xie L, Kang H, Xu Q, Chen MJ, Liao Y, Thiyagarajan M, et al. Sleep drives metabolite clearance from the adult brain. *Science* 2013;342:373-377

3. Iliff JJ, Wang M, Liao Y, Plogg BA, Peng W, Gundersen GA, et al. A paravascular pathway facilitates CSF flow through the brain parenchyma and the clearance of interstitial solutes, including amyloid β. *Sci Transl Med* 2012;4:147ra111

4. Zhou Y, Cai J, Zhang W, Gong X, Yan S, Zhang K, et al. Impairment of the glymphatic pathway and putative meningeal lymphatic vessels in the aging human. *Ann Neurol* 2020;87:357-369

5. Klostranec JM, Vucevic D, Bhatia KD, Kortman HGJ, Krings T, Murphy KP, et al. Current concepts in intracranial interstitial fluid transport and the glymphatic system: part II-imaging techniques and clinical applications. *Radiology* 2021;301:516-532

6. Taoka T, Masutani Y, Kawai H, Nakane T, Matsuoka K, Yasuno F, et al. Evaluation of glymphatic system activity with the diffusion MR technique: diffusion tensor image analysis along the perivascular space (DTI-ALPS) in Alzheimer's disease cases. *Jpn J Radiol* 2017;35:172-178

7. Bohr T, Hjorth PG, Holst SC, Hrabětová S, Kiviniemi V, Lilius T, et al. The glymphatic system: current understanding and modeling. *iScience* 2022;25:104987

8. Manduca A, Bayly PJ, Ehman RL, Kolipaka A, Royston TJ, Sack I, et al. MR elastography: principles, guidelines, and terminology. *Magn Reson Med* 2021;85:2377-2390

9. Hiscox LV, Schwarb H, McGarry MDJ, Johnson CL. Aging brain mechanics: progress and promise of magnetic resonance elastography. *Neuroimage* 2021;232:117889

10. Muthupillai R, Lomas DJ, Rossman PJ, Greenleaf JF, Manduca A, Ehman RL. Magnetic resonance elastography by direct visualization of propagating acoustic strain waves. *Science* 1995;269:1854-1857

11. Hiscox LV, Johnson CL, Barnhill E, McGarry MD, Huston J, van Beek EJ, et al. Magnetic resonance elastography (MRE) of the human brain: technique, findings and clinical applications. *Phys Med Biol* 2016;61:R401-R437

12. Murphy MC, Huston J 3rd, Ehman RL. MR elastography of the brain and its application in neurological diseases. *Neuroimage* 2019;187:176-183

13. Nanjappa M, Kolipaka A. Magnetic resonance elastography of the brain. *Magn Reson Imaging Clin N Am* 2021;29:617-630

14. Sack I, Beierbach B, Wuerfel J, Klatt D, Hamhaber U, Papazoglou S, et al. The impact of aging and gender on brain viscoelasticity. *Neuroimage* 2009;46:652-657

15. Sack I, Streitberger KJ, Krefting D, Paul F, Braun J. The influence of physiological aging and atrophy on brain viscoelastic properties in humans. *PLoS One* 2011;6:e23451

16. Arani A, Murphy MC, Glaser KJ, Manduca A, Lake DS, Kruse SA, et al. Measuring the effects of aging and sex on regional brain stiffness with MR elastography in healthy older adults. *Neuroimage* 2015;111:59-64

17. Hiscox LV, Johnson CL, McGarry MDJ, Perrins M, Littlejohn A, van Beek EJR, et al. High-resolution magnetic resonance elastography reveals differences in subcortical gray matter viscoelasticity between young and healthy older adults. *Neurobiol Aging* 2018;65:158-167

18. Lipp A, Trbojevic R, Paul F, Fehlner A, Hirsch S, Scheel M, et al. Cerebral magnetic resonance elastography in supranuclear palsy and idiopathic Parkinson's disease. *Neuroimage Clin* 2013;3:381-387

19. Runge JH, Hoelzl SH, Sudakova J, Dokumaci AS, Nelissen JL, Guenthner C, et al. A novel magnetic resonance elastography transducer concept based on a rotational eccentric mass: preliminary experiences with the gravitational transducer. *Phys Med Biol* 2019;64:045007

20. Guenthner C, Sethi S, Troelstra M, Dokumaci AS, Sinkus R, Kozerke S. Ristretto MRE: a generalized multi-shot GRE-MRE sequence. *NMR Biomed* 2019;32:e4049

21. Ehman EC, Rossman PJ, Kruse SA, Sahakian AV, Glaser KJ. Vibration safety limits for magnetic resonance elastography. *Phys Med Biol* 2008;53:925-935

22. Fovargue D, Kozerke S, Sinkus R, Nordsletten D. Robust MR elastography stiffness quantification using a localized divergence free finite element reconstruction. *Med Image Anal* 2018;44:126-142

23. Schmidt P, Gaser C, Arsic M, Buck D, Förschler A, Berthele A, et al. An automated tool for detection of FLAIR-hyperintense white-matter lesions in multiple sclerosis. *Neuroimage* 2012;59:3774-3783

24. Svensson SF, De Arcos J, Darwish OI, Fraser-Green J, Storås TH, Holm S, et al. Robustness of MR elastography in the healthy brain: repeatability, reliability, and effect of different reconstruction methods. *J Magn Reson Imaging* 2021;53:1510-1521

25. Arani A, Manduca A, Ehman RL, Huston Iii J. Harnessing brain waves: a review of brain magnetic resonance elastography for clinicians and scientists entering the field. *Br J Radiol* 2021;94:20200265

26. Sack I, Jöhrens K, Würfel J, Braun J. Structure-sensitive elastography: on the viscoelastic powerlaw behavior of in vivo human tissue in health and disease. *Soft Matter* 2013;9:5672-5680

27. Freimann FB, Müller S, Streitberger KJ, Guo J, Rot S, Ghori A, et al. MR elastography in a murine stroke model reveals correlation of macroscopic viscoelastic properties of the brain

with neuronal density. *NMR Biomed* 2013;26:1534-1539

28. Klein C, Hain EG, Braun J, Riek K, Mueller S, Steiner B, et al. Enhanced adult neurogenesis increases brain stiffness: in vivo magnetic resonance elastography in a mouse model of dopamine depletion. *PLoS One* 2014;9:e92582

29. Schregel K, Wuerfel E, Garteiser P, Gemeinhardt I, Prozorovski T, Aktas O, et al. Demyelination reduces brain parenchymal stiffness quantified in vivo by magnetic resonance elastography. *Proc Natl Acad Sci U S A* 2012;109:6650-6655

30. Guo J, Posnansky O, Hirsch S, Scheel M, Taupitz M, Braun J, et al. Fractal network dimension and viscoelastic powerlaw behavior: II. An experimental study of structure-mimicking phantoms by magnetic resonance elastography. *Phys Med Biol* 2012;57:4041-4053

31. Schwarb H, Johnson CL, McGarry MDJ, Cohen NJ. Medial temporal lobe viscoelasticity and relational memory performance. *Neuroimage* 2016;132:534-541

32. Guo J, Bertalan G, Meierhofer D, Klein C, Schreyer S, Steiner B, et al. Brain maturation is associated with increasing tissue stiffness and decreasing tissue fluidity. *Acta Biomater* 2019;99:433-442

33. Steward CE, Venkatraman VK, Lui E, Malpas CB, Ellis KA, Cyarto EV, et al. Assessment of the DTI-ALPS parameter along the perivascular space in older adults at risk of dementia. *J Neuroimaging* 2021;31:569-578

34. Bae YJ, Choi BS, Kim JM, Choi JH, Cho SJ, Kim JH. Altered glymphatic system in idiopathic normal pressure hydrocephalus. *Parkinsonism Relat Disord* 2021;82:56-60

35. Kikuta J, Kamagata K, Takabayashi K, Taoka T, Yokota H, Andica C, et al. An Investigation of water diffusivity changes along the perivascular space in elderly subjects with hypertension. *AJNR Am J Neuroradiol* 2022;43:48-55

36. Zhang W, Zhou Y, Wang J, Gong X, Chen Z, Zhang X, et al. Glymphatic clearance function in patients with cerebral small vessel disease. *Neuroimage* 2021;238:118257

37. Kedarasetti RT, Turner KL, Echagarruga C, Gluckman BJ, Drew PJ, Costanzo F. Functional hyperemia drives fluid exchange in the paravascular space. *Fluids Barriers CNS* 2020;17:52

38. Wang A, Wang R, Cui D, Huang X, Yuan L, Liu H, et al. The drainage of interstitial fluid in the deep brain is controlled by the integrity of myelination. *Aging Dis* 2019;10:937-948